Published in final edited form as:
Langmuir. 2010 September 7; 26(17): 13797–13804. doi:10.1021/la101740p.

Spontaneous Formation of Water Droplets at Oil-Solid Interfaces

Zhongqiang Yang and **Nicholas L. Abbott***
Department of Chemical & Biological Engineering, University of Wisconsin-Madison 1415 Engineering Drive, Madison, Wisconsin 53706, USA

Abstract

We report observations of spontaneous formation of micrometer-sized water droplets within micrometer-thick films of a range of different oils (isotropic and nematic 4-cyano-4'-pentylbiphenyl (5CB), and silicone, olive and corn oil) that are supported on glass substrates treated with octadecyltrichlorosilane (OTS) and immersed under water. Confocal imaging was used to determine that the water droplets nucleate and grow at the interface between the oils and OTS-treated glass with a contact angle of ~130°. A simple thermodynamic model based on macroscopic interfacial energetic arguments consistent with the contact angle of 130°, however, fails to account for the spontaneous formation of the water droplets. ζ-potential measurements performed with OTS-treated glass (− 59.0 ± 16.4 mV) and hydrophobic monolayers formed on gold films (2.0 ± 0.7 mV), when combined with the observed absence of droplet formation under films of oil supported on the latter surfaces, suggest that the charge of the oil-solid interface promotes partitioning of water to the interfacial region. The hydrophobic nature of the OTS-treated glass promotes dewetting of water accumulated in the interfacial region into droplets (a thin film of water is seen to form on bare glass). The inhibitory effect on droplet formation of both salt (NaCl) and sucrose (0.1mM to 500mM) added to the aqueous phase was similar, indicating that both solutes lower the chemical potential of the bulk water (osmotic effect) sufficiently to prevent partitioning of the water to the interface between the oil and supporting substrates. These results suggest that charged, hydrophobic surfaces can provide routes to spontaneous formation of surface-supported, water-in-oil emulsions.

Keywords

emulsions; interfaces; spontaneous emulsification; water droplets; interfacial droplets; octadecyltrichlorosilane (OTS); monolayers; liquid crystal; isotropic oil

Introduction

The formation of an emulsion from two immiscible fluids (e.g., oil and water) leads to the generation of interfacial area between the two fluids.[1,2] This generation of interfacial area requires that work be performed, typically through processes such as ultrasonication or mechanical agitation.[3] The resulting emulsions are kinetically stable, and surfactants are typically used to slow processes such as coalescence of the dispersed phase. In addition, however, processes that result in spontaneous emulsification have also been reported and such processes have substantial technological utility.[4–6] For example, the "Ouzo effect"[7,8] involves the addition of water to an oil that contains a solvent that is both water- and oil-soluble. The increase in water content of the oil-solvent mixture initiates the nucleation and

*Correspondence should be addressed to Nicholas L. Abbott (abbott@engr.wisc.edu, Fax: +1-608-262-5434).

Supporting Information Available: Additional experimental details. This material is available free of charge via the Internet at http://pubs.acs.org.

growth of oil droplets. Other methods, also based on solvent/solute diffusion between phases have been studied.9 Recently, interfacial oil droplets have also been made by forming emulsions in the bulk phase through the “Ouzo effect” and subsequently absorbing the oil droplets onto solid substrates.10,11 In this paper, we report observations that demonstrate that appropriately designed surfaces can be used to drive spontaneous formation of surface-supported water-in-oil emulsions (without any “Ouzo effect”). Because the droplets are surface-supported, surfactants are not required to slow coalescence.

The investigation that we report in this paper arose from observations made during studies of the ordering of micrometer-thick films of nematic liquid crystals (LCs), and ordering transitions induced in these thin films of nematic oil when placed into contact with aqueous phases containing a variety of adsorbates.12–22 In a typical experiment, a nematic film (thickness 20 μm) is formed on a hydrophobic substrate (e.g. octadecyltrichlorosilane (OTS)-treated glass) and then submerged under an aqueous phase. Through this process, LC-aqueous interface and a LC-solid interfaces are generated. Recently, when nematic 4-cyano-4’-pentylbiphenyl (5CB) was used as the LC and the supported LC film was immersed under distilled and deionized water, we observed water droplets to form spontaneously within the LC film. In this paper, we report on this phenomenon, and provide insights into the formation of this class of surface-supported water-in-oil emulsions.

We note that a number of recent studies have reported on the spontaneous formation of air bubbles (nanobubbles) at interfaces.23–26 These studies include observations of nanobubbles at interfaces between water and hydrophobic solids.23 The processes that give rise to the formation of the bubbles are not understood.24 For example, the large pressure differential calculated to exist across the bubble surface would be expected to result in collapse of the bubble in milliseconds.27 In contrast, experimental observations suggest that the bubbles are stable for hours.28 Although the phenomenon of nanobubble formation remains to be fully elucidated, there is accumulating evidence suggesting that nanobubbles may play a role in interfacial phenomena such as long-range attraction between hydrophobic solids,29,30 and slippage of simple fluids near a hydrophobic wall.31

Experimental Section

Materials

The glass microscope slides and coverslips (Fisher’s Finest Premium Grade), hydrogen chloride, methanol, methylene chloride, sucrose, hydrogen peroxide (30% w/v), sulfuric acid and silicone oil (Product No. S159-500), were obtained from Fisher Scientific (Pittsburgh, PA). Heptane, sodium chloride, octadecyltrichlorosilane (OTS), decanethiol ($C_{10}SH$), and hexadecanethiol ($C_{16}SH$) were obtained from Aldrich (Milwaukee, WI). 4-cyano-4’-pentylbiphenyl (5CB) was obtained from EM Sciences (New York, NY). Olive oil was obtained from Whole Foods Market (Austin, TX). Corn oil was obtained from ACH Food Companies Inc. (Memphis, TN). Vegetable oil was obtained from the J. M Smucker Company (Orrville, OH). Calcein AM was obtained from Invitrogen (Carlbad, CA). Ethanol was obtained from Aaper Alcohol and Chemical Co. (Shelbyville, KY). Deionization of a distilled water source was performed using a Milli-Q system (Millipore, Bedford, MA) to provide water with a resistivity of 18.2 MΩ cm. Gold grids (20 μm thickness, 333 μm pitch, and 55 μm bar width) were obtained from Electron Microscopy Sciences (Fort Washington, PA).

Preparation of Bare Glass

Glass microscope slides were cleaned with “piranha” solution (H_2SO_4/H_2O_2) according to published procedures.32

Preparation of Octadecyltrichlorosilane (OTS)-Treated Glass

Glass microscope slides were piranha cleaned and then coated with OTS, as described previously.32

Preparation of Gold Films

Films of titanium (thickness of 80 Å) and gold (thickness of 200 Å) were deposited onto piranha cleaned glass slides with an electron beam evaporator (VEC-3000-C manufactured by Tek-vac Industries, Brentwood, NY).33

Formation of Mixed Self-assembled Monolayers (SAMs) from Gold Films

Mixed SAMs were formed on the surfaces of the gold films by immersion into ethanolic solutions containing 0.8 mM $C_{10}SH$ and 0.2 mM $C_{16}SH$ for 2 h at 25 °C.34

Formation of Water Droplets

The gold specimen grids were placed onto the surfaces (5 mm × 25 mm) of solid substrates (either OTS-treated glass, bare glass or mixed SAMs formed from $C_{10}SH$ and $C_{16}SH$ on gold films). A drop of oil (e.g. 5CB, silicone oil, olive oil, corn oil or vegetable oil) was deposited into each the grid and the excess of oil was removed by using a 10 μL syringe (Fisher) in order to obtain a uniformly filled grid. The solid substrate supporting the gold grid was placed into 8 mL glass wells containing 5 mL distilled and deionized water. Parafilm (Menasha, WI) was placed over the top of the well to prevent evaporation of water. In some experiments, either NaCl or sucrose was dissolved into the water. Unless otherwise noted, the experiments were carried out at room temperature (25 °C).

Optical Characterization of Water Droplets

An Olympus BX60 microscope with a digital camera (Olympus C-2040 Zoom) was used to image the samples between crossed polars. Bright field images were obtained by removing the analyzer.

Fluorescent Imaging

An Olympus IX-71 inverted microscope equipped with Chroma Technology Corp. (Rockingham, VT) fluorescence filter cubes (ex/em 425–465 nm/485–533 nm) was used. Images were obtained with a Hamamatsu digital camera controlled by ImagePro software. A film of oil stabilized by a gold grid was placed on OTS-treated glass. The film was incubated under an aqueous phase for 3 or 6 days and then calcein AM (ex/em ~ 495 nm/ 515 nm) was added to a concentration of 2 μM. After incubation at room temperature in the dark for a day, the aqueous solution was exchanged with 300 mL water to remove excess of calcein AM in the bulk solution (keeping the aqueous-oil interface under the aqueous phase at all times).

Confocal Fluorescent Imaging

Confocal imaging was carried out at the W.M. Keck Laboratory for Biological Imaging at the University of Wisconsin-Madison. A film of 5CB stabilized by a gold grid was placed on OTS-treated glass. After the film was incubated under an aqueous phase containing 2 μM calcein AM for a week, the sample was exchanged with 300 mL water to remove excess of calcein AM from the bulk solution and then inverted over a coverslip and held a distance of 50 μm from the coverslip. The 5CB film was maintained under the aqueous phase during imaging. The samples were viewed with a Nikon A1RS Laser Scanning Confocal system (Melville, NY) using a 488 nm laser line to excite the calcein AM and an emission filter collecting 515 nm.

Contact Angle Measurements

Advancing (θ_a), receding (θ_r) and static (θ_s) contact angles of water were measured at room temperature using a goniometer (OCA 15 plus, software SCA20, Dataphysics Instruments). The contact angles reported in the manuscript are the average of three measurements. In addition, a water drop (~5 μL) was placed onto a substrate (OTS-treated glass or mixed monolayers) immersed under oil (silicone oil or 5CB) held in a transparent glass container. The average of three measurements was adopted as the static contact angle (θ_s) of water under oil.

Preparation of Gold Nanoparticles

200 μL of gold sol (diameter 150 nm) in aqueous solution (Ted Pella) was washed 3 times by (i) addition of 2 mL of distilled and deionized water, (ii) centrifugation at 4000 rpm for 15 min, and (iii) removal of the supernatant. The gold nanoparticles were then resuspended in 200 μL of water. An ethanolic solution containing 4 mM decanethiol and 4 mM hexadecanethiol was added to the gold particles, sonicated for 15 min, and allowed to incubate for 8 h. The nanoparticles were then washed 4 times in ethanol by centrifugation at 5000 rpm for 15 min. Particles were then dried in a vacuum and re-suspended in water by sonication for 15 mins.

Preparation of OTS-treated Silica Microparticles

100 μL of a dispersion of silica particles (diameter 2.3 μm, Bangs Labs) was treated with piranha solution, as described above for the cleaning of glass slides. The particles were washed in water, dried, and then functionalized with OTS as described above.

Measurements of Zeta Potential

Measurements of zeta potential were performed using a Zetasizer 3000HS (Malvern Instruments, Worcestershire, UK). The measurements were performed at ambient temperature using an applied voltage of 150 V. The Henry equation was used to calculate ζ-potentials from measurements of electrophoretic mobility.35

Results and Discussion

Our initial series of experiments sought to establish conditions under which aqueous droplets were observed to form within the supported films of oil. To this end, nematic 4-cyano-4’-pentylbiphenyl (5CB) was deposited into the pores (283 μm × 283 μm) of a 20 μm-thick gold electron microscopy grid. Each grid was supported on a glass microscope slide treated with octadecyltrichlorosilane (OTS). The OTS-treated glass anchors nematic phases of 5CB in an orientation that is perpendicular (homeotropic) to this interface. Following immersion under water, the film of nematic 5CB exhibited a bright optical appearance under crossed-polars, consistent with anchoring of the nematic LC in an orientation that was parallel to the aqueous interface (Figure 1A). The top row of images in Figure 1A are polarized light images (crossed polars) of the samples as a function of time, and the bottom row shows bright field images of the same samples. Inspection of the top row of images in Figure 1A reveals that the intensity of light transmitted through crossed-polars decreased over a period of several days. High magnification images shown in Figure 1B reveal that the decrease in intensity of the transmitted light was not due to a change in orientation of the LC but rather due to scattering of light from circular features that formed within the LC film.

To determine if these circular features were either water droplets or air bubbles, we carried out three experiments. First, a 5CB-filled grid supported on OTS-treated glass was immersed under water for seven days and circular objects were imaged within the sample.

Next, a partial vacuum was pulled over the surface of the water. The sizes of the circular objects were not changed by the partial vacuum, suggesting that the features were droplets of water and not air bubbles. Second, we incubated a 5CB-filled grid on OTS-treated glass in water under partial vacuum. The circular features were also observed to form under these conditions. Third, a 5CB-filled grid on OTS-treated glass was immersed into water for 3 days, and then the fluorescent dye calcein AM (water soluble) was added to a concentration of 2 μM. After one additional day of incubation of the system in the dark, bright, circular and fluorescent features were evident under the microscope (see Figure S1 of Supporting Information). This result, when combined with the other two experiments suggests that circular features seen in the images are water droplets and not air bubbles. These results also lead to two additional insights. First, these results indicate that calcein AM can diffuse from the aqueous phase into the droplets of water formed within the oil. Since calcein AM is charged and water-soluble, it is likely that calcein AM carries with it one or more waters of hydration. Second, we observed the formation of water droplets between the metallic grid and the OTS-treated glass (Figure S1). This result indicates that the grid is not in conformal contact with the OTS-treated glass, and that in some regions of the grid, at least, a film of 5CB separates the grid from the OTS-treated glass.

Next, we quantified the time-dependent growth of the droplets by image analysis. In a typical experiment, after a 6 h incubation in water, small dark spots were observed to form within the LC, corresponding to a droplet size of ~ 1.5 μm. The subsequent evolution of the population of drop sizes is shown in Figure 2. After incubation for one day, the droplets had grown to an average diameter of 4.0 μm with a standard deviation of 1.1 (indicated hereafter as ± Y). By day 3, the average droplet size was 8.0 ± 3.2 μm. We note that the change in size distribution of the droplets involved both continuous growth (presumably via molecular diffusion of water from the overlying aqueous phase) as well as discontinuous growth via coalescence of droplets within the LC film (see below for additional evidence in support of this conclusion). After seven days of incubation, the average droplet size was 16.8 ± 4.9 μm. The largest droplets that we observed were 30–40 μm in diameter, comparable in size to the thickness of LC film.

Figures S2–S4 of Supporting Information show the behaviors of the droplets during an additional 10 to 60 days of incubation. Interestingly, we observed that droplets which grew to have diameters of 30–40 μm over 10 days tended to disappear with further incubation. After they disappeared, new droplets were observed to form and grow again until they were 30–40 μm in size. We concluded that a dynamic and cyclical process of droplet growth and disappearance was occurring within the LC film (see Figure S4). The large droplets disappeared abruptly, suggesting that they likely fused with the bulk aqueous phase. The observation that the droplets disappeared when their diameters were comparable to the thickness of the LC film supports this proposition.

To provide additional insight into the evolution of the population of droplets in the LC film, we measured the number density of droplets in the LC film as a function of time (for 6 h and longer). Figure 3 shows that during the first 10 days, the number density of water droplets decreased approximately 10-fold, from $1.8 \times 10^4/mm^2$ to $1.3 \times 10^3/mm^2$. This decrease was due to coalescence of adjacent droplets (see Figure S5). Additional incubation of the samples (day 10 to day 30) led to a slight increase in the number density of droplets, a reflection of the disappearance of large droplets and reformation of multiple, small droplets, as discussed above. We also note that as the droplets grow and coalesce during incubation over 10 days, the regions of the OTS-treated glass adjacent to existing water droplets tended to not nucleate additional water droplets. This result suggests that the droplets of water supported on the OTS-treated glass may be depleting the concentration of water in the oil in

the vicinity of each droplet. Finally, we comment that control experiments (see Figure S6) confirmed that the properties of the OTS-treated glass did not change over time.

To determine the location and shape of the water droplets within the LC film, we used confocal fluorescence microscopy. The films of 5CB supported on OTS-treated glass were incubated in aqueous solutions containing 2 μM calcein AM (water soluble) for one week. As mentioned above, we observed water droplets formed under the LC films to contain calcein AM. Inspection of the confocal image shown in Figure 4 leads to two key conclusions. First, it is apparent that the water droplets formed in the 5CB are located at the interface between the nematic 5CB and OTS-treated glass. Second, it is evident that the contact angle formed by the water droplets at the interface is greater than 90°, although the exact values could not be determined due to uncertainty in the location of the edges of the droplets. Below we return to the characterization of the contact angles.

The results described above clearly establish that the features formed within the nematic 5CB in Figure 1 are water droplets that nucleate and grow from the interface between the nematic 5CB and OTS-treated glass. In order to determine if the nematic ordering of the 5CB plays a role in the formation of the droplets, we immersed 5CB supported on OTS-treated glass into water at 36 °C (nematic 5CB undergoes a phase transition to an isotropic phase at ~ 35.3 °C)36. At 36 °C, we observed water droplets to form within the isotropic phase of 5CB, suggesting that nematic order in the bulk of the film of 5CB is not necessary for droplet formation. We observed, however, that during seven days of incubation at 36 °C, the growth rate of droplets in isotropic 5CB was faster than that in nematic 5CB at 25 °C (see Figure S7). The higher growth rate of the droplets at 36 °C is likely due to (i) the higher solubility of water in the isotropic 5CB as compared to nematic 5CB; (ii) the higher rates of diffusion of water at the elevated temperatures, and/or (iii) accelerated rates of droplet coalescence at the elevated temperatures37,38.

We also comment that a number of recent studies have demonstrated that the nematic order of 5CB can lead to interactions between particles dispersed in the LC. The interactions are due to particle-induced elastic strain of the LC as well as formation of topological defects in the LC. These LC-mediated interactions are anisotropic, long-ranged and ~ 1000 times stronger than van der Waals forces typically encountered in colloidal systems with isotropic solvents. These LC-mediated forces lead to a variety of self-assembled structures, such as linear chains and two-dimensional arrays of particles.39–41 We considered it possible that nematic forces may lead to the ordering of the water droplets formed in nematic 5CB. Our analysis of the organization of water droplets in the nematic films has not, to date, revealed any such evidence of long-range ordering induced by nematic forces.

The results above suggest that nematic order within the bulk of the 5CB films is not necessary to induce formation of the water droplets. Although bulk nematic order is not needed, the experiments do not rule out a role for interfacial ordering of mesogens, as has been observed in Langmuir film studies of 5CB and 8CB.42 To determine the generality of the phenomenon shown in Figure 1, we performed a series of experiments using isotropic oils, including silicone oil, olive oil, corn oil and vegetable oil. Our results (Figure 5) revealed that water droplets formed in all of these isotropic oils (Figure S8 and S9). Differences measured in the rates of growth of the droplets shown in Figure S9 likely reflect differences in the solubility of water in the various oils (e.g. silicone oil (~ 200 ppm),43 olive oil (~ 900 ppm),44 corn oil (~ 200 ppm),44 vegetable oil (~ 200 ppm)44 and 5CB (~ 720 ppm / 40 mM)).45,46

Next we sought to determine if macroscopic interfacial energy arguments could provide an explanation for the thermodynamic driving force leading to the formation of the droplets. As

shown in Figure 6, the initial state of the system was taken to be the oil film supported on the OTS-treated glass immersed under water. In Figure 6, γ is the interfacial tension and θ is the contact angle of the water droplet in oil on the OTS-treated glass. The initial surface energy E_i of the OTS-oil interface with area A_1 shown in Figure 6 is

$$E_i = A_1 \gamma_{OTS-oil} \tag{1}$$

After formation of the water droplet, the newly formed interface between water and oil is A_2, and the final surface energy is:

$$E_f = A_1 \gamma_{OTS-water} + A_2 \gamma_{water-oil} \tag{2}$$

The difference in surface energy between the final and initial state is thus:

$$\Delta E = A_1 \gamma_{OTS-water} + A_2 \gamma_{water-oil} - A_1 \gamma_{OTS-oil} \tag{3}$$

Division of Eq. (3) by area $A_1\gamma_{water-oil}$, gives:

$$\frac{\Delta E}{A_1 \gamma_{water-oil}} = \frac{\gamma_{OTS-water} - \gamma_{OTS-oil}}{\gamma_{water-oil}} + \frac{A_2}{A_1} \tag{4}$$

By using Young's equation47

$$\cos\theta = \frac{\gamma_{OTS-oil} - \gamma_{OTS-water}}{\gamma_{water-oil}} \tag{5}$$

a relationship between A_1, A_2 and θ can be derived as (see Figure S10)

$$\frac{A_2}{A_1} = \frac{2(1-\cos\theta)}{\sin^2\theta} \tag{6}$$

Substitution of Eq. (5) and (6) into Eq. (4) yields

$$\frac{\Delta E}{A_1 \gamma_{water-oil}} = \left(\frac{2(1-\cos\theta)}{\sin^2\theta} - \cos\theta\right) \tag{7}$$

To determine if Eq. (7) can account for the spontaneous formation of the water droplets, we measured the contact angle of water immersed under 5CB, when supported on OTS-treated glass (Table 1). The contact angle was determined to be ~ 130°. Substitution of this value into the right hand side of Eq. (7) yields 6.17. This leads to the conclusion that ΔE is positive and thus the spontaneous formation of water droplets observed in our experiments (Figure 1) can not be described within the framework of the above-described macroscopic model. Indeed, for all non-zero values of contact angles, ΔE is positive.

To provide additional insight into the factors controlling the formation of the water droplets, we carried out a series of experiments to determine how the surface properties of the supporting solid substrates influenced droplet formation. We investigated three substrates that differed in surface charge and wettability: OTS-treated glass, bare glass, and gold films supporting monolayers formed from alkanethiols ($C_{10}SH$ and $C_{16}SH$). Table 1 shows that

the contact angles of water droplets are similar when measured on the OTS-treated glass and mixed monolayers formed on the gold films. In contrast, water completely wets the bare glass (cleaned). Past studies have extensively characterized these surfaces, and it has been established that OTS-treated glass and bare glass possess substantial densities of negative surface charges. For example, it has been reported that glass modified with *n*-hexadecyltrichlorosilane (HC-16) possesses a ζ-potential of ~ − 50 mV when immersed under water.48 Our measurements (see Methods section) revealed that silica microparticles coated with OTS possess a ζ-potential of − 59.0 ± 16.4 mV in water. The origin of the surface charge density giving rise to the ζ-potential is believed to be residual silanol groups, a conclusion that is consistent with the effects of pH on ζ-potentials of OTS-treated substrates.49,50 In contrast, we measured gold nanoparticles functionalized with mixed monolayers of $C_{10}SH$ and $C_{16}SH$ to have ζ-potentials of ~ 2.0 mV.

Figure 7 compares films of 5CB supported on the above-described three substrates, when immersed under water. For comparison, Figure 7A and B shows the formation of water droplets on OTS-treated glass after two days of incubation. Interestingly, when bare glass was used, as shown in Figure 7C and D, “islands” of water were observed to form (see also Figure S11). The bare glass is hydrophilic and we speculate that as water accumulates at the oil-solid interface, the water wets the bare glass and forms a discontinuous film instead of forming droplets with contact angle > 90° (as seen on OTS-treated glass). In contrast, experiments performed with mixed monolayers formed from $C_{10}SH$ and $C_{16}SH$ on gold films did not reveal evidence of droplet formation (see Figure 7E and F; see also Figure S12 for additional observations). Similarly, water droplets were not observed to form in a film of silicone oil that was supported on the mixed monolayer formed on gold (details in Figure S13). Here we emphasize that the contact angle of water measured on the mixed monolayer formed from $C_{10}SH$ and $C_{16}SH$ on gold is similar to contact angle measured using OTS-treated glass (Table 1); whereas use of the latter surface led to droplet formation, the former one did not. These results, when combined with the observation of water film formation on bare glass, strongly suggest that the surface charge of the substrate supporting the oil film plays a central role in promoting the formation of the water droplets at the interface.

Many past studies of LC films submerged under aqueous solutions containing buffering salts and electrolytes have been reported, and these studies have not described the formation of water droplets within the supported LC films.12¯14,16,32,51 The absence of any prior reports of formation of water droplets within LC films led us to speculate that the phenomenon reported in this paper may be influenced by the presence of ions within the aqueous phase. In order to determine if the droplet formation described in this paper is suppressed by the presence of solutes added to the aqueous phase, we incubated 5CB supported on OTS-treated glass in aqueous phases containing either NaCl or sucrose (Figure 8 and Figure S14 and S15). Inspection of Figure 8 reveals that the presence of increasing concentrations of solutes in the aqueous phase decreases the size of the droplets formed in the LC film after three days. At concentrations of solutes greater than 200 mM, we did not observe the formation of aqueous droplets in the LC film. We make two observations regarding these results. First, the influence of the NaCl on droplet formation is very similar to sucrose, thus suggesting that the effect of the solute is osmotic in nature and not related to ionic strength. Second, the effect of the solutes at concentrations below ~200 mM was to slow the formation of droplets and not to stop the growth of the droplets at a given size.

The results described above, when combined, lead to the following overall understanding of the droplet formation process, which is summarized as having three stages (Figure 9). The initial state of the system (stage 1) comprises oil (nematic 5CB or isotropic oils) films supported on either OTS-treated glass, bare glass or mixed monolayer formed from $C_{10}SH$

and $C_{16}SH$ on gold film, and then immersed under water. At stage 1, there exists an oil-water interface and an oil-solid interface.

When the system reaches stage 2 of the droplet formation process (see Figure 9), the sites of negative charge at the interfaces defined by either bare or OTS-treated glass have adsorbed water that has diffused across the LC film from the bulk aqueous phase. The silanol groups that remain after cleaning and reaction with OTS are the likely origins of the surface charge. Because the dielectric constant of water (80.1)52 is larger than 5CB ($\varepsilon_{\|}$ = 18.5 and $\varepsilon_{\perp}$ = 7.0), 53 the water will preferentially partition towards the charges immobilized on the interface (charge-dipole attraction).54 Past studies have established that the solubility of water in 5CB is ~ 40 mM,45›46 and that the diffusion coefficients of a range of small molecules are approximately 10^{-11} m^2/s.55 Thus, the diffusion time for a small molecule such as water across a 20μm-thick film of nematic 8CB is approximately 6 secs. This characteristic diffusion time is many orders of magnitude smaller than the time that characterizes the appearance and growth of the water droplets (~ 1 day, see Figure 1). We note, however, that the initial states of the droplets are nanoscopic, and thus the droplets on OTS-treated glass must grow over a period of hours to be observed by optical microscopy. In contrast, for the case of bare glass, the water forms island-like films instead of dewetting into droplets. In contrast to either the OTS-treated glass or bare glass substrates, the interfaces defined by the mixed monolayers formed from $C_{10}SH$ and $C_{16}SH$ on gold do not possess a surface charge density that is comparable in magnitude to the glass substrates (see above for ζ-potential measurements). The driving force for adsorption of water onto the mixed monolayer on the gold film is, therefore, minimal.

The final stage of the process leading to the formation of the droplets (stage 3) corresponds to times longer than 6 h incubation. During stage 3, the water droplets formed at the interface are sufficiently large to be observed by optical microscopy. Water molecules diffuse continuously from the bulk aqueous phase through the oil to reach the oil-solid interface and oil-water droplet interface, resulting in droplet growth and coalesce. The number of droplets on the interface decreases with increasing time of incubation due to droplet coalescence that accompanies droplet growth (see Figure S4 and 5). The droplets grow until their size approaches the thickness of the oil film; at this point, they bridge the oil film and fuse with the bulk aqueous film. The fusion event is followed by the nucleation and growth of additional droplets at the oil-solid interface, thus leading to a cyclical process that occurs for > 60 days. Finally, we comment that our measurements of the influence of solutes on droplet formation are consistent with the above-described process. In brief, the addition of solutes lowers the chemical potential of the water in the bulk aqueous solution to an extent that prevents its partitioning to the charged interfaces of the substrates.

The process of droplet formation described in this paper is spontaneous following the placement of the solid-supported oil film under water. When the substrate is OTS-treated glass, our results indicate that the initial state of the system (stage 1 in Figure 9) is not the equilibrium state. Although we clearly establish that spontaneous formation of water droplets takes place at the solid-oil interface over a period of days, our results to do not unambiguously establish the equilibrium state of the system. Remarkably, over a period of ~ 60 days, we observed the experimental system to go through a series of cycles involving the nucleation and growth of water droplets at the solid-oil interface followed by fusion of the droplets with the bulk aqueous phase. During this period of spontaneous droplet formation, no external work is performed on the system. The results reported in this paper can, therefore, be viewed as a type of spontaneous emulsification (leading to surface-supported, water droplets).

Conclusions

In conclusion, we report experimental observations of spontaneous formation water droplets at oil-solid interfaces. Two key factors appear to be necessary for the process to occur: the charge density of the solid substrate needs to be high (the ζ-potential of the OTS-treated glass interface used in our study was −59.0 ± 16.4 mV) and the macroscopic contact angles of the water droplets on the surface need to be sufficiently large to cause dewetting of water under the oil (we measured contact angles of water under oil on the OTS-treated glass to be ~130°). Our results support the proposition that water diffuses through the oil and partition to the regions of the interface between the oil and solid with high charge density. A continuous film of water is not, however, formed at the OTS-treated glass interface due to the high contact angle of the water on the surface under the oil. This physical picture is supported by the observation that droplet formation can be suppressed either by (i) using surfaces with low surface charge densities (mixed monolayers of alkanethiols on films of gold) or (ii) by adding solutes to the bulk aqueous phase that lower the chemical potential of the water and thus prevent partitioning of the water across the oil to the oil-solid interfacial region. In addition to providing fundamental insights into the behaviors of surface-supported oil films immersed under water, our study suggests that appropriately designed surfaces can be used to promote spontaneous formation of emulsions. Because the emulsions formed by this phenomenon are surface-supported, they are not prone to coalescence to the same extent as unsupported emulsions.

Supplementary Material

Refer to Web version on PubMed Central for supplementary material.

Acknowledgments

We thank Lance Rodenkirch from the W.M. Keck Laboratory for Biological Imaging at the University of Wisconsin-Madison for assistance with confocal fluorescent imaging. We cheerfully thank Daniel Abras, I-Hsin Lin, Aaron M. Lowe, Yiqun Bai, Jacob T. Hunter and Santanu K. Pal, Gary M. Koenig Jr., Chad A. Hladilek and Gaurav Pranami for technical assistance and helpful discussions. This work was partially supported by the National Science Foundation (DMR-0520527 and DMR-0602570) and National Institutes of Health (CA108467 and CA105730), and the ARO (W911NF-07-1-0446 and W911NF-06-1-0314).

References

1. Tadros, TF. Emulsion Science and Technology. Wiley; 2009.
2. Leal-Calderon, F.; Schmitt, V.; Bibette, J. Emulsion Science: Basic Principles. Springer; 2007.
3. Wedlock, DJ. Controlled Particle, Droplet and Bubble Formation. Oxford: Butterworth-heinemann Ltd; 1994.
4. Miller, CA. Spontaneous Emulsification: Recent Developments with Emphasis on Self-Emulsification. In Emulsions and Emulsion Stability. Taylor and Francis London; 2006.
5. Anton N, Benoit JP, Saulnier P. J. Controlled Release. 2008; 128:185.
6. Anton N, Vandamme TF. Int. J. Pharm. 2009; 377:142. [PubMed: 19454306]
7. Vitale SA, Katz JL. Langmuir. 2003; 19:4105.
8. Ganachaud F, Katz JL. Chem. Phys. Chem. 2005; 6:209. [PubMed: 15751338]
9. Davies, JT.; Rideal, EK. Interfacial Phenomena. New York and London: Academic Press; 1961.
10. Zhang XH, Ducker W. Langmuir. 2008; 24:110. [PubMed: 18044934]
11. Zhang X, Wei X, Ducker W. Langmuir. 2010; 26:4776. [PubMed: 20099815]
12. Kinsinger MI, Sun B, Abbott NL, Lynn DM. Adv. Mater. 2007; 19:4208.
13. Lockwood NA, Gupta JK, Abbott NL. Surf. Sci. Rep. 2008; 63:255.
14. Park JS, Abbott NL. Adv. Mater. 2008; 20:1185.

15. Price AD, Schwartz DK. J. Am. Chem. Soc. 2008; 130:8188. [PubMed: 18528984]
16. Brake JM, Daschner MK, Luk YY, Abbott NL. Science. 2003; 302:2094. [PubMed: 14684814]
17. Gupta JK, Tjipto E, Zelikin AN, Caruso F, Abbott NL. Langmuir. 2008; 24:5534. [PubMed: 18419143]
18. Meli MV, Lin IH, Abbott NL. J. Am. Chem. Soc. 2008; 130:4326. [PubMed: 18335929]
19. Price AD, Ignes-Mullol J, Vallve MA, Furtak TE, Lo YA, Malone SM, Schwartz DK. Soft Matter. 2009; 5:2252.
20. Bahr C. Phys. Rev. E. 2006; 73 030702.
21. McCamley MK, Ravnik M, Artenstein AW, Opal SM, Zumer S, Crawford GP. J. Appl. Phys. 2009; 105:123504.
22. Brake JM, Abbott NL. Langmuir. 2002; 18:6101.
23. Tyrrell JWG, Attard P. Phys. Rev. Lett. 2001; 87:176104. [PubMed: 11690285]
24. Zhang XH, Maeda N, Craig VSJ. Langmuir. 2006; 22:5025. [PubMed: 16700590]
25. Borkent BM, Dammer SM, Schonherr H, Vancso GJ, Lohse D. Phys. Rev. Lett. 2007; 98:204502. [PubMed: 17677702]
26. Wang YL, Bhushan B. Soft Matter. 2010; 6:29.
27. Ljunggren S, Eriksson JC. Colloids Surf. A. 1997; 129–130:151.
28. Yang J, Duan J, Fornasiero D, Ralston J. J. Phys. Chem. B. 2003; 107:6139.
29. Attard P. J. Phys. Chem. 1989; 93:6441.
30. Parker JL, Claesson PM, Attard P. J. Phys. Chem. 1994; 98:8468.
31. Wang Y, Bhushan B, Zhao X. Langmuir. 2009; 25:9328. [PubMed: 19572534]
32. Brake JM, Abbott NL. Langmuir. 2002; 18:6101.
33. Skaife JJ, Abbott NL. Chem. Mater. 1999; 11:612.
34. Drawhorn RA, Abbott NL. J. Phys. Chem. 1995; 99:16511.
35. Hunter, RJ. Zeta Potential in Colloid Science. New York: Academic Press; 1981.
36. Park JWB, C S, Labes MM. J. Am. Chem. Soc. 1975; 97:4398.
37. Bibette, J.; Leal-Calderon, F.; Schmitt, V.; P, P. Springer Tracts in Modern Physics: Emulsion Science. Basic principles. Berlin: Springer-Verlag; 2002.
38. Sing AJF, Graciaa A, Lachaise J, Brochette P, Salager JL. Colloids Surf., A. 1999; 152:31.
39. Muševič I, Škarabot M. Soft Matter. 2008; 4:195.
40. Poulin P, Stark H, Lubensky TC, Weitz DA. Science. 1997; 275:1770. [PubMed: 9065396]
41. Musevic I, Skarabot M, Tkalec U, Ravnik M, Zumer S. Science. 2006; 313:954. [PubMed: 16917058]
42. Zhang Z, Zheng DS, Guo Y, Wang HF. Phys. Chem. Chem. Phys. 2009; 11:991. [PubMed: 19177218]
43. Liland, KB.; Eidnes, K.; Bjørneklett, K.; Hvidsten, S. Measurement of solubility and water content of insulating oils for HV XLPE Cable Terminations. IEEE International Symposium on Electrical Insulation; Vancouver, BC, Canada. 2008.
44. Chaiyasit W, Elias RJ, McClements DJ, Decker EA. Crit. Rev. Food Sci. Nutr. 2007; 47:299. [PubMed: 17453926]
45. Kimura NUJ, Hayashi S, Takenaka T. J. Mol. Struct. 1984; 116:153.
46. Shah RR, Abbott NL. J. Am. Chem. Soc. 1999; 121:11300.
47. Young T. Philos. Trans. R. Soc. 1805; 95:65.
48. Lin C-H, Chaudhury MK. Langmuir. 2008; 24:14276. [PubMed: 19053623]
49. Shyue J-J, De Guire MR, Nakanishi T, Masuda Y, Koumoto K, Sukenik CN. Langmuir. 2004; 20:8693. [PubMed: 15379494]
50. Lin Y-C, Yu B-Y, Lin W-C, Chen Y-Y, Shyue J-J. Chem. Mater. 2008; 20:6606.
51. Gupta JK, Meli MV, Teren S, Abbott NL. Phys. Rev. Lett. 2008; 100 048301.
52. The CRC Handbook of Chemistry and Physics. CRC; 2009.
53. Cummins PG, Dunmur DA, Laidler DA. Mol. Cryst. Liq. Cryst. 1975; 30:109.

54. Shamai R, Andelman D, Berge B, Hayes R. Soft Matter. 2008; 4:38.
55. Han S, Martin SM. J. Phys. Chem. B. 2009; 113:12696. [PubMed: 19715323]

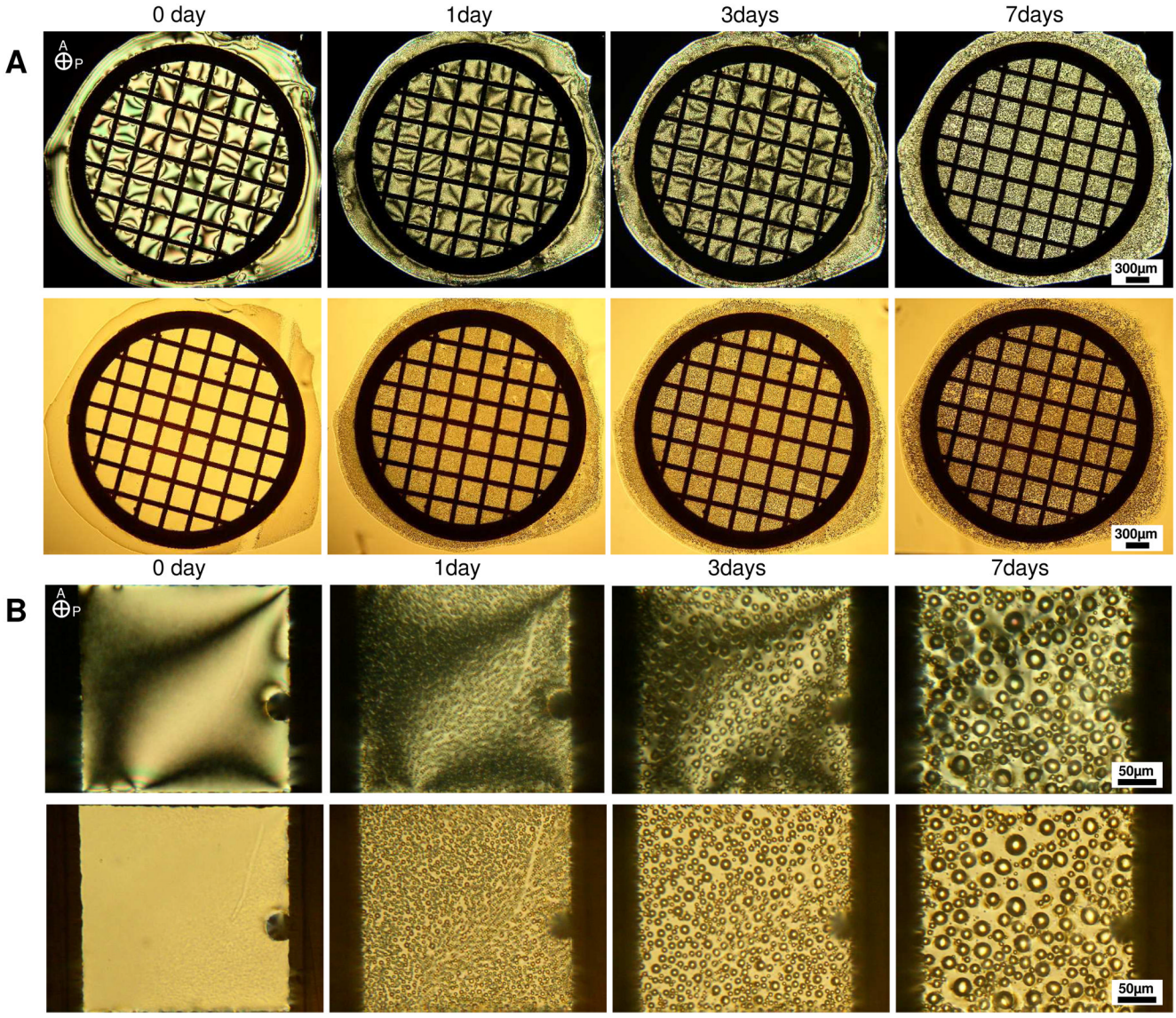

Figure 1.

Optical micrographs of nematic 5CB hosted in gold grids supported on OTS-treated glass slides in contact with water for seven days at (A) low and (B) high magnification, respectively. The top rows in (A) and (B) are polarized light images (crossed polars) and the bottom rows are bright field images.

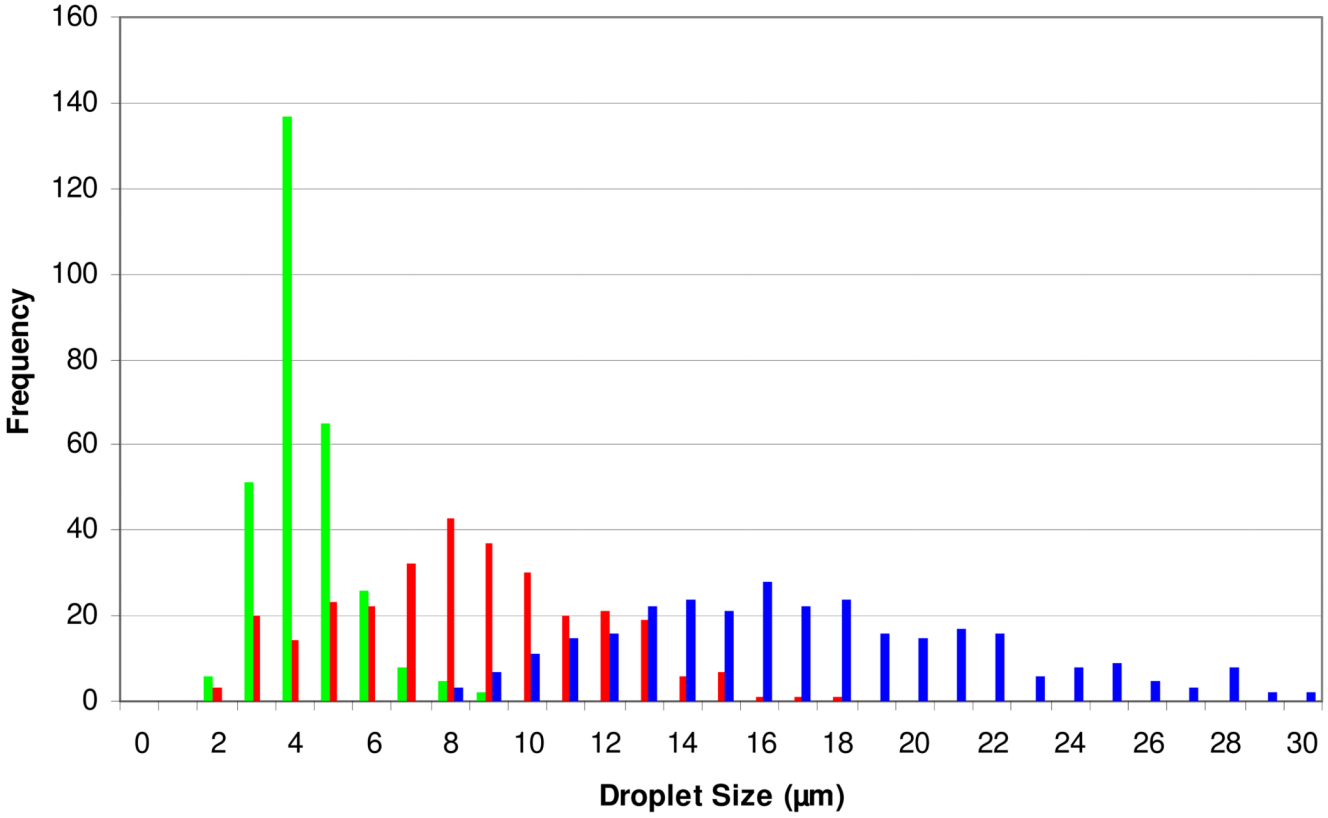

Figure 2.
The distribution of sizes of water droplets formed in films of nematic 5CB supported on OTS-treated glass. The results were obtained at room temperature, and the green, red and blue columns represent droplet size distributions measured after 1, 3 and 7 days, respectively, of incubation under water.

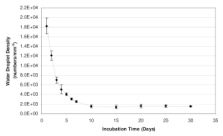

Figure 3.
The number density of water droplets formed under films of nematic 5CB supported on OTS-treated glass that were incubated under water at room temperature.

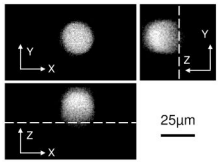

Figure 4.
Confocal fluorescent images of a single water droplet formed within nematic 5CB supported on OTS-treated glass: The XY axes indicated in the images lie within the plane of the OTS-treated glass interface, and the Z axis lies along the surface normal. The dashed white line shows the location of the OTS-treated glass interface.

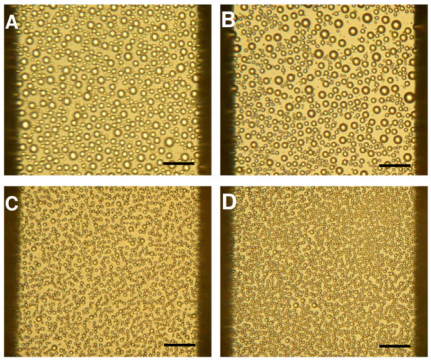

Figure 5.
Optical micrographs of formation of water droplets at the OTS-treated glass interface when using isotropic oils: (A) silicone oil; (B) olive oil; (C) corn oil and (D) vegetable oil. The images were obtained after 7 days of immersion under water at room temperature. The scale bar corresponds to 50 μm.

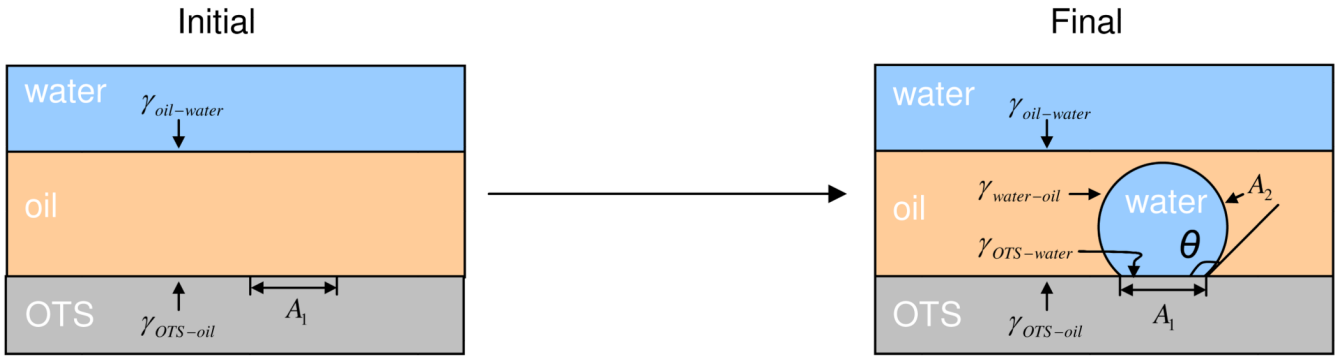

Figure 6.
Schematic illustration of the experimental system before (left) and after (right) formation of a water droplet at the interface between the oil and OTS-treated glass.

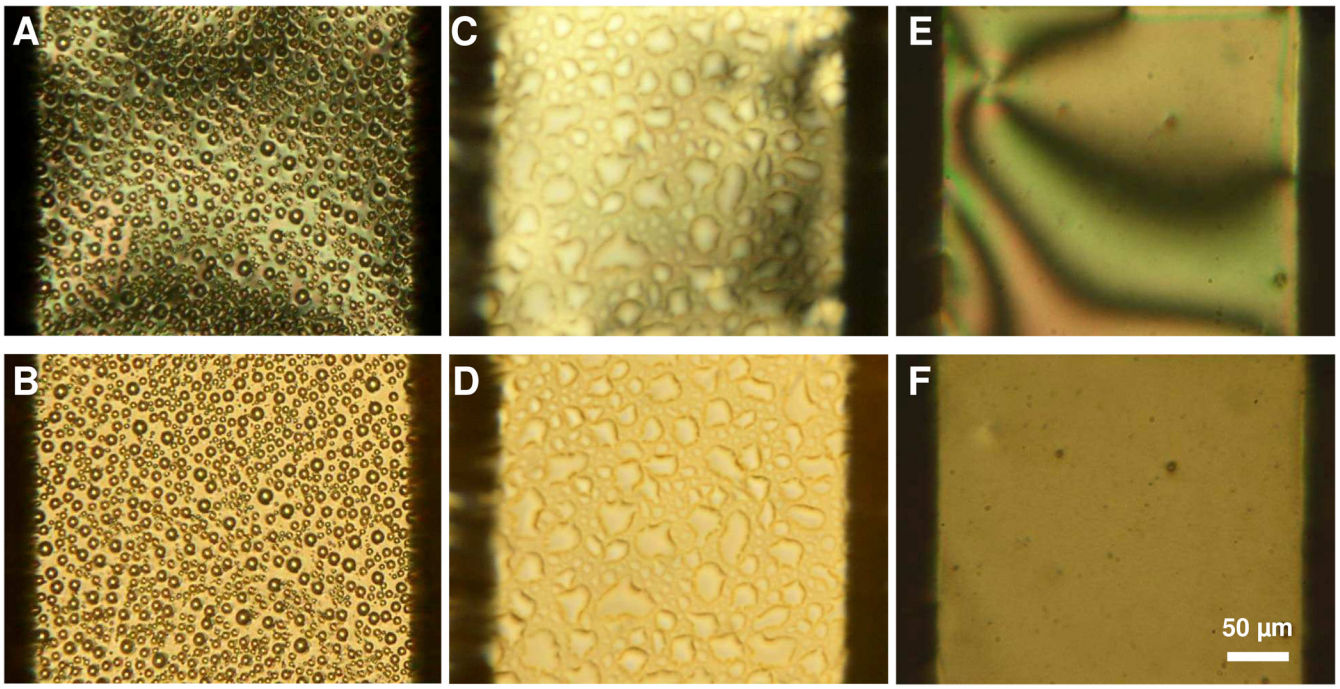

Figure 7.
Optical micrographs of films of nematic 5CB incubated under water for two days. The film of 5Cb was supported on: (A, B) OTS-treated glass; (C, D) bare glass; (E, F) mixed monolayers formed from $C_{10}SH$ and $C_{16}SH$ on gold film. The images in the top row are polarized light images (cross polars) and the images in the bottom row are bright field images.

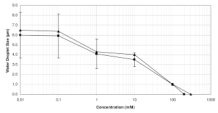

Figure 8.

Influence of solute concentration on the size of water droplets formed at the interface between 5CB and OTS-treated glass. The films of 5CB were immersed for 3 days under aqueous solutions of either NaCl (■) or sucrose (▲). The experiments were performed at room temperature.

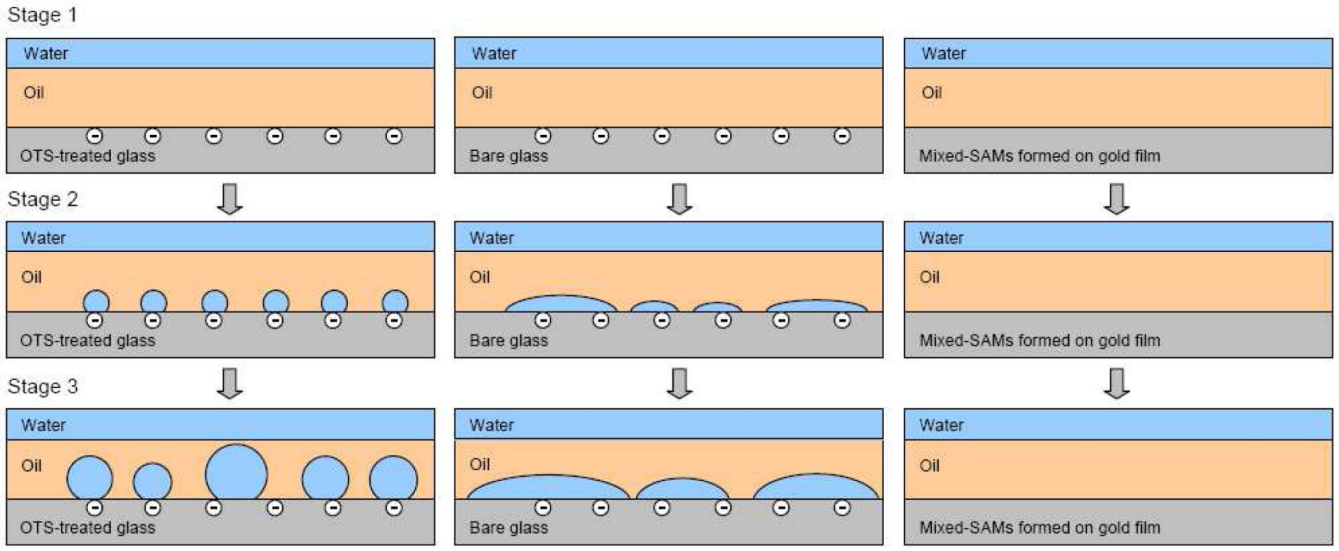

Figure 9.

Schematic illustration of the processes (3 stages) occurring with films of oil supported on three substrates (immersed under water): (left) OTS-treated glass; (middle) bare glass and (right) mixed monolayers formed from $C_{10}SH$ and $C_{16}SH$ on gold films. The illustrations are not drawn to scale.

Table 1

Advancing (θ_a), receding (θ_r) and static (θ_s) contact angles of water measured on either OTS-treated glass or mixed monolayers of $C_{10}SH$ and $C_{16}SH$ formed on gold films. The contact angles of water were measured under silicone oil, 5CB or air (indicated below as the medium).

Substrate	Medium	θ_a (°)	θ_r (°)	θ_s (°)
OTS-treated glass	silicone oil	–	–	131 ± 3
	5CB	–	–	127 ± 5
	air	101 ± 1	86 ± 2	98 ± 1
Mixed monolayers ($C_{10}SH$, $C_{16}SH$)	silicone oil	–	–	146 ± 3
	5CB	–	–	134 ± 5
	air	103 ± 2	95 ± 1	99 ± 2